Quantum properties and applications of 2D Janus crystals and their superlattices

Cite as: Appl. Phys. Rev. **7**, 011311 (2020); https://doi.org/10.1063/1.5135306
Submitted: 07 November 2019 • Accepted: 06 January 2020 • Published Online: 21 February 2020

M. Yagmurcukardes, Y. Qin, S. Ozen, et al.

Applied Physics Reviews REVIEW scitation.org/journal/are

Quantum properties and applications of 2D Janus crystals and their superlattices

Cite as: Appl. Phys. Rev. **7**, 011311 (2020); doi: 10.1063/1.5135306
Submitted: 7 November 2019 · Accepted: 6 January 2020 ·
Published Online: 21 February 2020

M. Yagmurcukardes,[1,a)] Y. Qin,[2] S. Ozen,[3] M. Sayyad,[2] F. M. Peeters,[1] S. Tongay,[2,a)] and H. Sahin[3,a)]

AFFILIATIONS

[1]Department of Physics, University of Antwerp, Groenenborgerlaan 171, B-2020 Antwerp, Belgium
[2]Materials Science and Engineering, School of Engineering for Matter, Transport, and Energy, Arizona State University, Tempe, Arizona 85281, USA
[3]Department of Photonics, Izmir Institute of Technology, 35430 Izmir, Turkey

[a)]**Authors to whom correspondence should be addressed:** Mehmet.Yagmurcukardes@uantwerpen.be; sefaattin.tongay@asu.edu; and hasansahin@iyte.edu.tr

ABSTRACT

Two-dimensional (2D) Janus materials are a new class of materials with unique physical, chemical, and quantum properties. The name "Janus" originates from the ancient Roman god which has two faces, one looking to the future while the other facing the past. Janus has been used to describe special types of materials which have two faces at the nanoscale. This unique atomic arrangement has been shown to present rather exotic properties with applications in biology, chemistry, energy conversion, and quantum sciences. This review article aims to offer a comprehensive review of the emergent quantum properties of Janus materials. The review starts by introducing 0D Janus nanoparticles and 1D Janus nanotubes, and highlights their difference from classical ones. The design principles, synthesis, and the properties of graphene-based and chalcogenide-based Janus layers are then discussed. A particular emphasis is given to colossal built-in potential in 2D Janus layers and resulting quantum phenomena such as Rashba splitting, skyrmionics, excitonics, and 2D magnetic ordering. More recent theoretical predictions are discussed in 2D Janus superlattices when Janus layers are stacked onto each other. Finally, we discuss the tunable quantum properties and newly predicted 2D Janus layers waiting to be experimentally realized. The review serves as a complete summary of the 2D Janus library and predicted quantum properties in 2D Janus layers and their superlattices.

TABLE OF CONTENTS

I. INTRODUCTION TO JANUS MATERIALS

The name "Janus" comes from the ancient Roman god of beginnings and transitions which has two faces, one looking to the future while the other facing the past. The use of the "Janus" term in the scientific community dates back to 1988 when Casagrande and his co-workers fabricated glass beads. These beads had hydrophobic

properties on one side and hydrophilic features on the other; thus, the term Janus was coined.[1] Following this work, the use of Janus has expanded gradually and is now commonly used to describe materials that have two vastly different chemical compositions and sometimes functionalities on each side.

As shown in Fig. 1, if the material in question is a zero-dimensional (0D) Janus nanoparticle, top and bottom (north and south) hemispheres consist of different compositions. However, it must be mentioned that the exact definition of Janus or what it describes in the nanoparticle community is rather broad and is not confined to north/south poles, which will be clarified later in the review. This Janus concept in 0D nanoparticles (NPs) gradually expanded into the 1D nanowires and, more recently, to the 2D materials communities as these new classes of materials became available. Currently, the term Janus or "polar" can be commonly found in the 0D and 1D materials community, whereas it is in its beginning for 2D materials.

What is the rationale behind designing and synthesizing such challenging materials? The direct answer is the added functionalities and the new physical, chemical, and quantum phenomena arising from the broken symmetry. As we will show in this review article, breaking the mirror symmetry in materials creates added functionalities, and it is an effective way to engineer the material properties, even unlock new physics. Because of these opportunities and new functionalities, creating new materials by the Janus concept is a growing field, which is the central justification for this timely review article. Due to recent exciting developments in the field of quantum materials, the main focal point of this review article will be on Janus 2D materials and quantum material systems. Furthermore, we will summarize recent discoveries in 0D and 1D Janus materials to give the reader a sufficient context and depth in the field. We want to invite those who are interested in 0D Janus NPs to consult other great review articles that appeared in the last two decades.[6–10]

First, an overview of Janus nanoparticles is presented in Sec. II in terms of the different synthesis techniques and their possible applications. Section III is devoted to experimental and theoretical reports on Janus structures of graphene derivatives (Sec. III A), group-VI (excitonic) 2D Janus TMDs (Sec. III B), other types of Janus TMDs (Sec. III C), and vdW superlattices of Janus layers (Sec. III D). After introducing the fundamentals of these materials, Sec. IV is devoted to their tunable quantum properties. In Sec. V, we present other types of 2D Janus materials that extend beyond TMDs, and the review article is summarized in Sec. VI.

II. JANUS NANOPARTICLES

A. Classical vs Janus nanoparticles

The classical nanoparticles refer to simple single-composition particles such as Au NPs, TiO_2 NPs, and quantum dots. The material

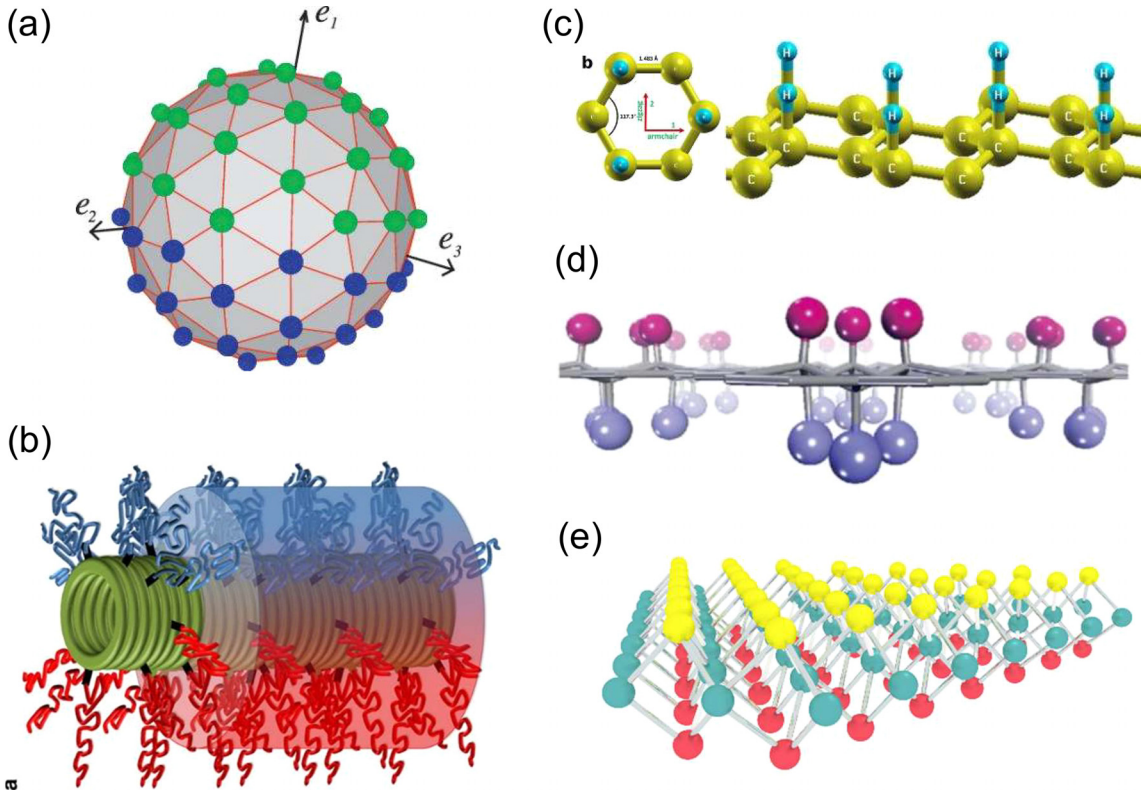

FIG. 1. Different types of Janus materials are schematically shown for the following: (a) 0D nanoparticles: Reprinted with permission from A. Kharazmi and N. V. Priezjev, J. Chem. Phys. **142**(23), 234503 (2015). Copyright 2015 AIP Publishing.[2] (b) 1D nanotubes: Reprinted with permission from Danial *et al.*, Nat. Commun. **4**, 2780 (2013). Copyright 2013 Springer Nature.[3] (c) and (d) 2D graphene derivative: Reprinted with permission from Zhang *et al.*, Nat. Commun. **4**, 1443 (2013). Copyright 2013 Springer Nature.[4] Reprinted with permission from Peng *et al.*, Nanoscale **7**(22), 9975–9979 (2015). Copyright 2015 Royal Society of Chemistry.[5] (e) 2D transition metal dichalcogenides (TMDs) (selenium atoms are depicted with yellow, metal atoms with cyan, and sulfur atoms with red).

properties of these classical NPs are mostly defined by surface-to-volume ratios, particle geometries, composition, and surface functionalization groups. After large nanoscience and nanotechnology initiatives in the last few decades, these classical nanoparticles have found several real-life applications ranging from cosmetics to cancer therapy and biosensing/detection.

While classical NPs are geometrically uniform, the Janus NPs display more complex structure. Just like the Roman god Janus, they typically have two faces; thus, their internal symmetry is broken. However, the term Janus is not a sufficient adjective to scientifically define the NPs. From a geometrical standpoint, 0D Janus nanoparticles can be divided into various categories, namely, spherical, dumbbell-like, half raspberry-like, cylindrical, disk-like, or other creative shapes and forms (Fig. 2). It is important to note that these geometrical differences manifest themselves in the physical behavior of Janus NPs and sometimes offer entirely different applications.

Interaction between the compartments of different Janus NPs gives rise to broad possibilities for self-assembly of novel microstructures. For example, reversible cluster formation and size control could be achieved with pH trigger.[15] A combination of dual characters in the Janus NPs structure also allows for innovative functionalities that cannot be realized in traditional NPs systems. With hydrophilic and hydrophobic features coexisting, particulate surfactant-like behavior was observed for Janus NPs with different morphologies.[16–18] Muller *et al.* also showed compatibilization of immiscible polymers (polystyrene and poly-methyl methacrylate) with Janus NPs aligning between different polymer domains.[19,20] Duo functionalities in Janus NPs also enabled their biological applications. Studies have shown successful binding to cell membranes with one side of Janus nanoparticle and the introduction of imaging ability from the other side.[20] Simultaneous imaging and magnetolytic therapy was achieved with polystyrene-magnetite nanoparticles.[21]

B. The synthesis of Janus NPs

Those Janus NPs can be fabricated by many different synthesis techniques such as surface coating by deposition of evaporated metal particles,[22,23] layer-by-layer self-assembly,[24,25] and photo-polymerization.[13,26] A typical example of Janus nanoparticles synthesized by electrodeposition technique is shown in Fig. 2. Importantly, each Janus nanoparticle type has its unique properties, which were demonstrated to be useful in various applications. For example, while polymeric nanoparticles were found to be suitable for surfactants, inorganic ones can be used in drug delivery, bioimaging, and biomarker. On the other hand, polymeric-inorganic Janus nanoparticles were fabricated as

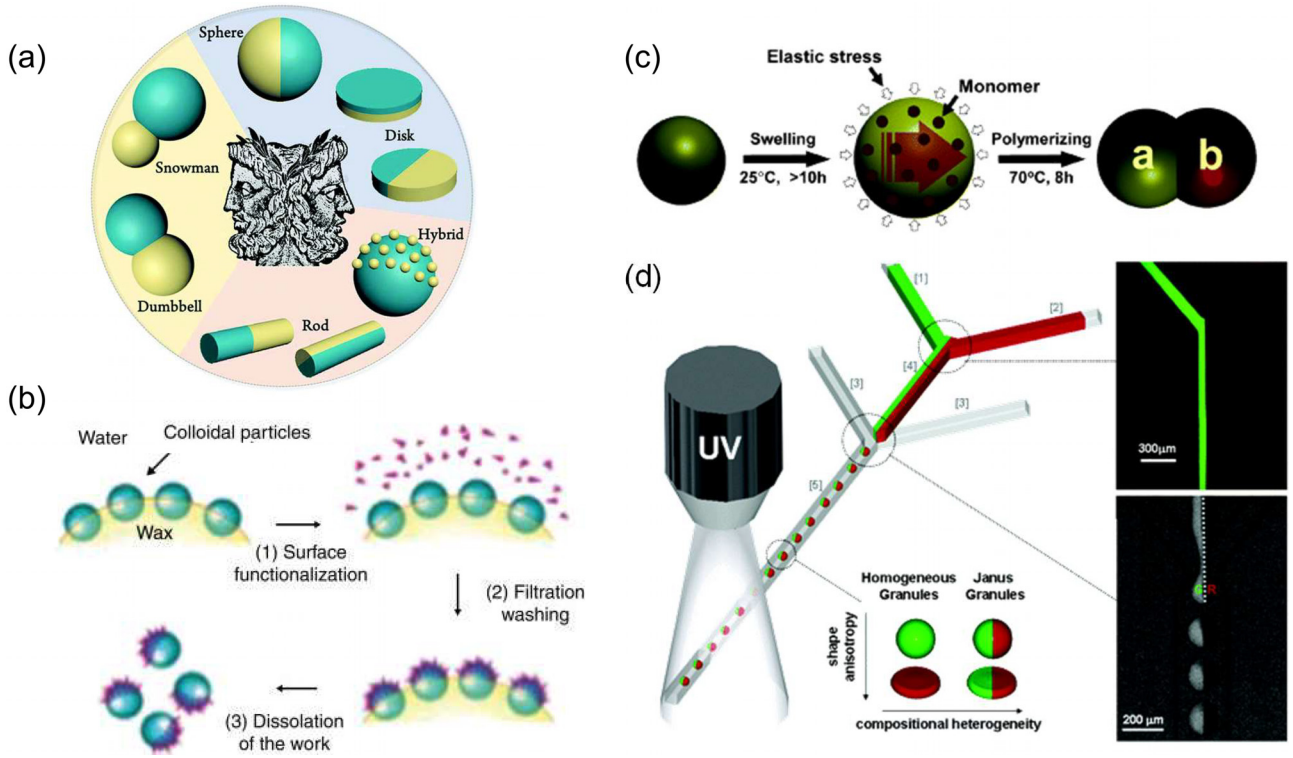

FIG. 2. (a) Variety of different types of 0D and 1D Janus materials.[11] Reprinted with permission from Zhang *et al.*, Biomater. Sci. **7**(4), 1262–1275 (2019). Copyright 2019 Royal Society of Chemistry. (b)–(d) summarize some of the common Janus material synthesis techniques employed in the field.[12–14] Reprinted with permission from Perro *et al.*, Colloids Surf. A **332**(1), 57–62 (2009). Copyright 2009 Royal Society of Chemistry. Reprinted with permission from Shepherd *et al.*, Langmuir **22**(21), 8618–8622 (2006). Copyright 2006 American Chemical Society. Reprinted with permission from Kim *et al.*, J. Am. Chem. Soc. **128**(44), 14374–14377 (2006). Copyright 2006 American Chemical Society.

functional coatings or films, serving as building blocks for novel devices and materials.

III. TWO-DIMENSIONAL JANUS CRYSTALS

After the successful synthesis of graphene,[27] the first single-layer crystal made of carbon, other atomically thin materials, and their heterostructures have been the focus of interest in materials science, physics, and chemistry.[28–38] Confinement of electrons, holes, and excitations in the out-of-plane direction leads to dramatic changes in their physical and chemical properties. Recent experimental developments have opened up the way to synthesize Janus two dimensional (2D) single-layer materials. Researchers demonstrated the successful fabrication of a Janus type single-layer MoSSe structure by the controllable exchange of S by Se at one surface of a MoS_2 layer or Se by S at $MoSe_2$ layer.[39,40] The fact that having the two surfaces of a 2D material made out of different atoms enriches the functionality of the material that can be useful in developing novel nanodevices in the fields of chemistry, biology, and physics. Regarding the growing research interest in 2D Janus single-layer structures, here we review the recent experimental and theoretical progress in the development of Janus single-layers, including their structural, vibrational, electronic, optical, and mechanical properties.

A. Graphene-based Janus layers

Since the first example of a 2D monolayer was graphene, the first example of 2D Janus layers is naturally graphene-based. The very first studies of *graphane* were purely theoretical inspired from graphene, which is essentially hydrogenated graphene with H bonded on both sides of the carbon sheet.[41,42] Following the theoretical prediction of *graphane* sheets, Zhou *et al.*[42] have shown that it is theoretically possible to realize hydrogen decorations specifically on one side of graphene, or it is possible to remove H atoms from one side of *graphane*. The resulting structure was named *graphone*. This is the first example of a 2D Janus layer, which had two different surface configurations.

One of the exciting aspects of this new Janus material is that it was predicted to be a ferromagnetic indirect bandgap semiconductor, which was quite visionary for its time. It also offered new ways to introduce ferromagnetism in 2D, which is advantageous over other strategies such as substitutional doping, nanoribbons creation, or vacancy generation. Later, Haberer *et al.* first demonstrated the isolation of partially hydrogenated single-sided graphene (see Fig. 3), which was observed to have the C_4H composition, via hydrogen plasma treatment of gold-supported chemical vapor deposited (CVD) graphene.[43] The impact of the single-sided hydrogenated graphene was reported to be its wide bandgap, which is suitable for optoelectronic applications in the UV range.

Single-sided graphene functionalization or "*2D single-side graphene Janus layers*" did not stay limited to *graphone* but extended to different surface functionalization groups, like halogens such as Cl and F. Yang *et al.* reported that Cl atoms tend to adsorb onto the graphene surface and form p-type doped, single-sided chlorinated graphene structures.[45] Depending on the charge transfer between the adsorbed Cl atoms, it was shown that two alternative structural formations could occur: Cl atoms can be adsorbed on para-site C atoms resulting in maximum coverage of 25%, or two Cl atoms interact with each other to form Cl_2 molecules and desorb from the graphene surface. Moreover, the electronic band structure indicated the tunable bandgap of chlorinated graphene ranging from 0 eV to 1.3 eV. The first experimental observation of asymmetrically halogenated graphene was reported by Robinson *et al.* through the single-side fluorination of graphene.[46] By exposing a CVD-grown graphene sheet on Cu foil to a XeF_2 atmosphere, it was demonstrated that the F coverage is almost saturated at 25%, yielding the formation of a C_4F structure which was reported to be optically transparent and over 6 orders of magnitude more resistive than a graphene monolayer.

In addition to *2D single-side graphene Janus layers*, other functionalization directions were taken toward creating asymmetrical Janus structures or "*2D asymmetric graphene Janus layers*." These materials involved two different types of atoms on each side of graphene. Singh and Bester predicted the stable formation of hydrofluorinated structures in which C atoms are saturated by either H or F atoms at the two different surfaces.[47] It was reported that the adsorption configuration of the H and F atoms plays a crucial role in the electronic bandgap of the structure. For the most stable composition, the two sides of graphene were modified homogenously with H or F atoms; Yang *et al.* further extended the prediction to various halogen atoms.[44] As shown in Fig. 3, their findings indicated that the electronic bandgap increases as the difference between the atomic radii of the two adsorbed atoms is larger. Notably, the formation of asymmetric single-layers using graphene as the basis material was also reported

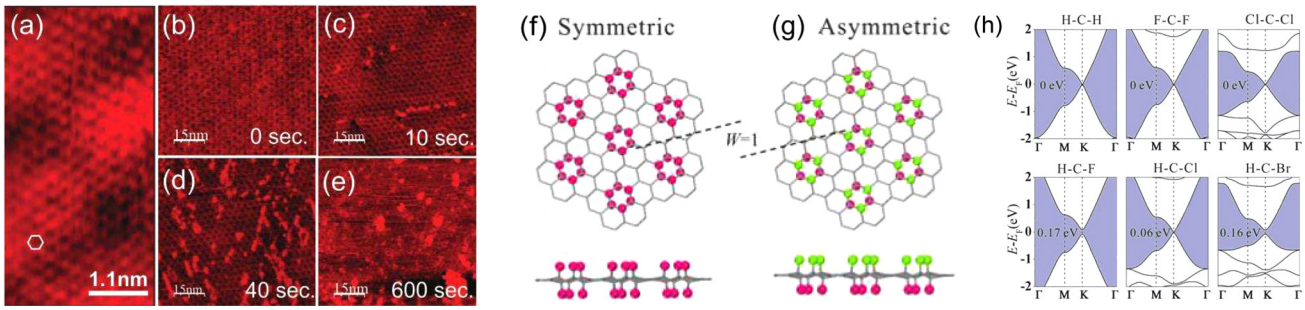

FIG. 3. (a)–(e) STM images collected from 2D Janus graphene layers at different hydrogenation times.[43] Reprinted with permission from Haberer *et al.*, Adv. Mater. **23**(39), 4497–4503 (2011). Copyright 2011 John Wiley and Sons. (f) Symmetric as well as (g) asymmetric (Janus) arrangements of surface modified graphene layers.[44] (h) Calculated band structures of different types of symmetric and Janus graphene layers.[44] Reprinted with permission from Yang *et al.*, J. Appl Phys. **113**(8), 084313 (2013). Copyright 2013 AIP Publishing.

with modification of the graphene surface by small molecules, functional polymers, or deposition of nanoparticles.[44]

At the height of graphene excitement, 2D graphene-based Janus layers mostly had one goal in mind: to introduce an electronic bandgap. Thus, most of the theory work focused on changes in the electronic structure and experiment focused on the synthesize route. Possible emergent quantum phenomena or potential vertical polarization field-induced changes still remain nearly unknown. With the renewed interest in 2D Janus transition metal dichalcogenides (TMDs), graphene-based Janus materials might lead to new insights and research directions in the upcoming years.

B. Transition metal dichalcogenide based Janus layers

1. Janus transition metal dichalcogenides

Two-dimensional transition metal dichalcogenides (TMDs) are another class of 2D materials with the general chemical formula of MX_2 where M is the transition metal (M = Nb, Ti, Ta, Mo, etc.) and X represents the chalcogen group elements S, Se, or Te. To date, 2D TMDs have shown many exotic quantum phenomena such as superconductivity, charge density waves, Weyl fermions, excitonics, and valleytronics.[48] Similar to graphene-based Janus layers, TMDs have been predicted to form Janus TMDs layers by replacing one side of the material with a different type of chalcogen atoms. More specifically, if the top sulfur layer of a MoS_2 2D sheet is stripped and replaced by selenium, it creates a MoSSe Janus layer, as shown in Figs. 1(e) and 4(a).[49] At the time of writing this review article, the majority of the fundamental studies on Janus TMDs are all theory-based, and experimental characterization efforts are lacking, perhaps due to considerable difficulties in sample preparation. There are two synthesis articles from 2017 focusing on Janus MoSSe,[39,40] but no other synthesis efforts on these materials are available to realize other Janus chalcogenide systems. Nevertheless, the existing theory articles point toward rather exciting quantum phenomena arising from broken mirror symmetry. Below, we summarize some of these extraordinary properties.

2. Emergent quantum phenomena in 2D Janus TMDs

Among 2D single-layer materials, classical TMDs are an emerging class of materials owing to their wide-ranging electronic properties from metallic to semiconducting and even to superconducting, which offer opportunities for various applications.[50,51] MoS_2, for example, has been shown to undergo band renormalization going from bulk to monolayers[51] and shows an indirect to direct bandgap transition in the monolayer limit. Spin–orbit coupling (SOC) and lack of inversion symmetry in its structure lead to coupled spin and valley behavior, but overall zero out of plane potential gradience forbids Rashba splitting in bulk form, which could allow for spintronics and valleytronics application.[49,52,53]

The idea for breaking the internal symmetry of a TMD single-layer was first proposed by Cheng *et al.* by predicting the stability of polar single-layer TMDs, which were recently named as Janus TMDs after their successful synthesis.[49] Proposed Janus TMDs MXY (M = Mo or W and X, Y = S, Se, or Te) comply with the same crystal structure with their parent material: metal atoms are sandwiched between two layers of chalcogen atoms, and together they form a hexagonal lattice. The Janus monolayer structure evolves from TMD by completely replacing one layer of chalcogen atoms with another group VI element. Given the broken mirror symmetry, the point group of monolayer changes from D_{3h} in TMDs to C_{3v} in Janus. The electronegativity difference between the top and bottom layer elements leads to asymmetric dipole distribution, which results in a "*colossal vertical electric field*" within the monolayer of the Janus structure [see Figs. 4(a) and 4(b)]. As a result of the polarization field, the top and the bottom layers of the Janus sheets have different potential energies, which have been predicted to be as high as 0.5 eV, as shown in Fig. 4(b). In this section, we will discuss the emerging quantum effects arising from the intrinsic vertical polarization field and the broken mirror symmetry.

a. Rashba–Dresselhaus splitting. Rashba spin–orbit coupling refers to the fact that an electron moving in the 2D electric field will experience an effective magnetic field that is coupled to its spin. Spin

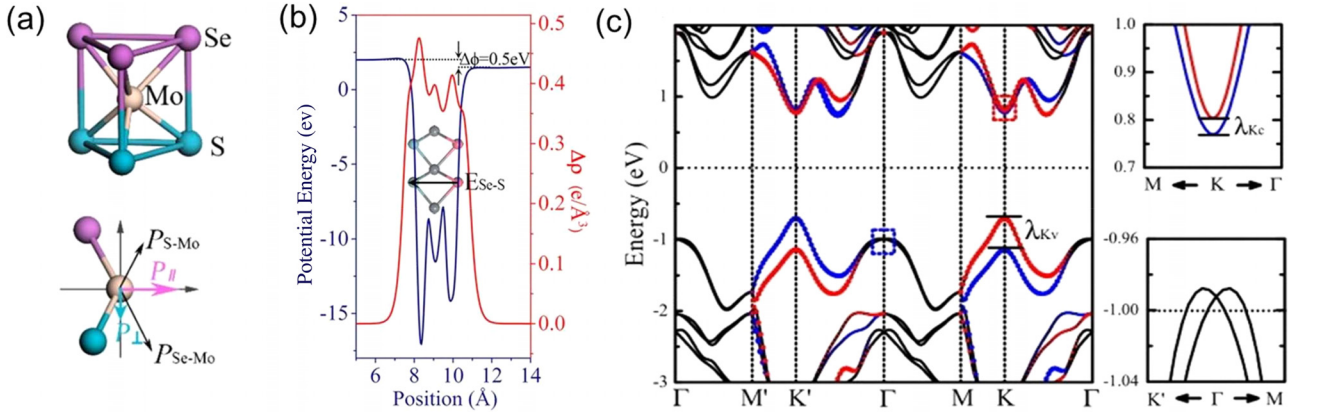

FIG. 4. (a) 2D Janus TMDs and induced polarization are shown schematically.[54] Reprinted with permission from Li *et al.*, J. Phys. Chem. Lett. **10**(3), 559–565 (2019). Copyright 2019 American Chemical Society. (b) Across the 2D Janus layers, the potential energy and the charge density change differently compared to classical TMDs; it induces colossal polarization field and work function difference between the two sides of the 2D Janus layers.[55] Reprinted with permission from Li *et al.*, J. Phys. Chem. Lett. **8**(23), 5959–5965 (2017). Copyright 2017 American Chemical Society. (c) As a result of this polarization field, the band structure splits at the Γ point, which is known as Rashba splitting.[49] Reprinted with permission from Cheng *et al.*, Europhys. Lett. **102**(5), 57001 (2013). Copyright 2013 IOP Publishing, Ltd.

degeneracy is lifted in systems with such effect, which potentially allows spin manipulation and electron trajectory control for spin–orbitronic applications.[56] In TMDs such as MoS_2, inversion asymmetry introduces spin-momentum locking, and the energy dispersion shows two parabolas that are shifted by a momentum offset. However, this could only be observed when a surface state or an external out-of-plane field is present in the crystal. By manually breaking mirror symmetry through chalcogen alternation, an intrinsic out-of-plane polarization field is exerted on the structure. This polarization has been shown to stabilize spin-nondegenerate states at the Γ point and induce "*Giant Rashba splitting*."[49,57,58] This splitting is shown in the band structure in Fig. 4(c). According to the theoretical predictions, the Rashba splitting parameters can be much larger than those of other champion materials such as BiTeI.[57] Interestingly, Rashba parameters can be further tuned by in-plane strain engineering to reach rather impressive values.[58,59] While results are still at theory level, massive Rashba tunable spin splitting parameters are particularly useful for spintronics and quantum device applications since spins can be selectively accessed and manipulated on demand.

b. Magnetism and skyrmionics. Discovery of ferromagnetism in monolayer CrI_3[49,60] and bilayer $CrGeTe_3$[61] at low temperature shows that magnetism ordering can be stabilized in 2D systems, which dramatically broadens electronic applications of van der Waals materials. Other 2D systems, including VSe_2,[62,63] $MnSe_2$,[63] and Fe_3GeTe_2,[64,65] were later proven to show near room temperature ferromagnetism down to the monolayer limit. Here, 2D Janus layers enrich this quantum phenomenon owing to its intrinsic permanent dipole moment and colossal vertical polarization field.

Current theory articles on Janus VSSe[66,67] and CrIBr[67] layers show that the intrinsic polarization enables high Curie temperature (T_c) ferromagnetism in these materials. However, these studies are mainly based on density functional theory (DFT) parameters and simple Bohr magneton per unit cell argument; thus, the fundamental understanding of how the magnetic order in 2D change under extreme polarization field in Janus layers remains unknown. One creative work, however, points out that one effect of the polarization field is the direct change in the Dzyaloshinskii–Moriya interaction (DMI) strength. More specifically, their calculations show that DMI interaction changes in Janus MnSeTe and MnSTe and pave its way to potentially stabilize topologically protected skyrmions (magnetic textures or particle-like knots) which opens another pathway for quantum spin manipulation (Fig. 5).[68,69]

c. Novel excitonic and valleytronic phenomena. The lack of inversion symmetry, together with large spin–orbit coupling (SOC), is already known to give 2D TMDs such as $MoSe_2$, WSe_2, or WS_2 individually controllable valleys in K-space at the K and K′ points in the first Brillouin zone.[70] As a result of the unique combination of spin and valley degrees of freedom, optically generated electrons and holes are both valley- and spin-polarized (spin-valley locking), a quantum property that is absent in other traditional semiconductors.

Here the broken mirror symmetry and the presence of a permanent dipole offer fascinating physics and even directions into quantum applications. While the entire findings are theory-driven, early predictions show that Janus layers contain excitons and their homojunction of Janus TMDs is capable of forming type-II junctions with band offsets comparable to the potential difference between the top and the bottom faces of the Janus sheets [Figs. 6(a)–6(c)]. More interestingly, depending on the stacking order, the valleytronic responses [Figs. 6(d) and 6(e)] can be greatly tuned, and colossal Berry curvature values are also possible (∼100 $bohr^2$). These properties are quite noteworthy and open up opportunities to achieve 100% valley polarization without any need for magnetic-electric fields or electronic doping/gating.[59,71,72] This offers completely new ways to tune the spin polarization ratio (valleytronics) without using external electric or magnetic fields.

d. Colossal vertical piezoelectricity. Following the fabrication of single-layer Janus MoSSe, Dong *et al.* investigated the large in-plane and out-of-plane piezoelectric properties of single-layer Janus TMDs through first-principles calculations.[73] It was reported that the weak out-of-plane piezoelectric coefficient of single-layer Janus MXY (M = Mo or W and X, Y = S, Se, or Te) could be significantly enhanced by strain [Fig. 6(e)]. In multilayer structure, the piezoelectric property is boosted, and it is tunable by layer stacking sequence. Moreover, it was shown that the improved out-of-plane piezoelectric coefficient of multilayer MXY is more significant than that of commonly used bulk piezoelectric materials.

3. Single-layer Janus TMDs: Experimental realization

The first experimental synthesis of 2D Janus single-layers was reported by two independent groups simultaneously in 2017,

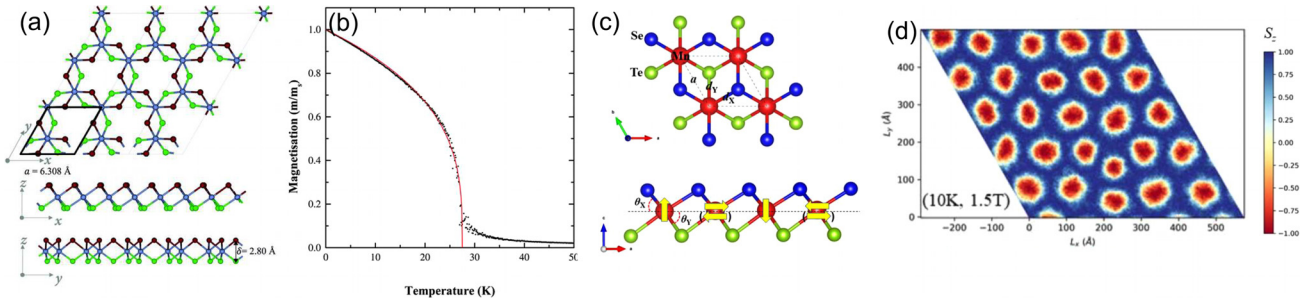

FIG. 5. (a) Janus 2D magnetic trihalides and (b) the predicted magnetism at different temperature.[67] Reprinted with permission from Moaied *et al.*, Phys. Chem. Chem. Phys. **20**(33), 21755–21763 (2018). Copyright 2018 Royal Society of Chemistry. (c) One of the novel emergent quantum phenomena in 2D Janus magnetic layers is the formation of skyrmions.[68] (d) Spin textures in the presence of a large polarization field and enhanced DMI interactions.[68]

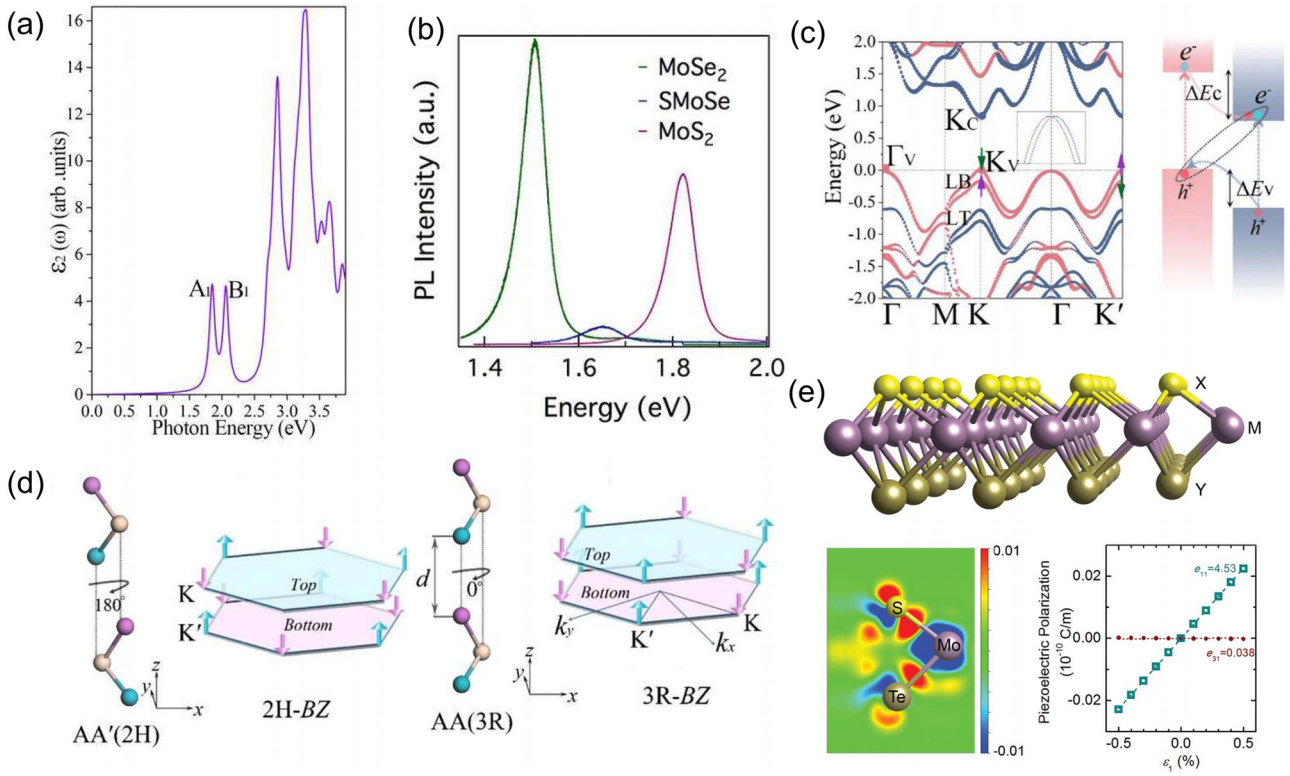

FIG. 6. (a) and (b) The predicted excitonic absorption[55] and measured PL spectra[39] of MoSSe excitonic Janus layers. Reprinted with permission from Li *et al.*, J. Phys. Chem. Lett. **8**(23), 5959–5965 (2017). Copyright 2017 American Chemical Society. Reprinted with permission from Zhang *et al.*, ACS Nano **11**(8), 8192–8198 (2017). Copyright 2017 American Chemical Society. (c) Aside from single layers, bilayer homojunction Janus layers have been shown to yield type-II heterojunctions owing to the inherent polarization field.[54] (d) Depending on the stacking type and order, it has been predicted that valleytronic properties dramatically change.[54] Reprinted with permission from Li *et al.*, J. Phys. Chem. Lett. **10**(3), 559–565 (2019). Copyright 2019 American Chemical Society. (e) Piezoelectricity with respect to strain in 2D Janus TMDs.[73] Reprinted with permission from Dong *et al.*, ACS Nano **11**(8), 8242–8248 (2017). Copyright 2017 American Chemical Society.

but no other synthesis efforts appeared ever since, presumably due to difficulties in synthesis approaches. Both techniques involved high-temperature processing and relied on replacing the top layer chalcogens with a different chalcogen either by thermal effects or plasma treatment. Li and his co-workers reported on a strategy for the experimental growth of Janus TMDs single-layers[40] which start with synthesis of monolayer MoS_2 flakes on a sapphire substrate using the chemical vapor deposition (CVD) method. In a two-step process, the top sulfur layer of single-layer MoS_2 was replaced by H-atoms in plasma, and then replacement of H atoms by Se atoms was achieved by thermal selenization (see Fig. 7). In this work, the effect of temperature on the selenization process was investigated, and 350–450 °C temperature range was recommended. Above this temperature, it was shown that 2D alloys could be formed due to the thermal energy provided during the functionalization step.

In another study, Zhang *et al.* also claimed single-layer Janus MoSSe[39,40] formation. In contrast to the experiment performed by Li and his co-workers,[40] Zhang *et al.* used single-layer $MoSe_2$ as the base layer, and the top Se layer was replaced by S atoms at very high temperatures (750 °C). Even though the Raman spectra match to those predicted from theory, it remains unclear how alloying can be prevented at such high temperatures. In these two studies, the presence of Janus layers was confirmed mainly by comparing the calculated phonon dispersion relation with the measured Raman spectrum and room temperature PL spectra were also provided to show light emission from these layers.

However, it remains unknown how excitonic effects in these materials influence the results at low temperatures. More importantly, it appears that reproducing these results is not straightforward, as evidenced by lack of experimental verification since 2017. This suggests that the growth mechanism is highly complex and possibly depends on a variety of growth parameters including flow rate, sample positioning, temperature window, plasma power, initial material quality, and many other parameters related to the kinetics of the reaction. More experimental results and possibly other innovative methods are needed to push the limit in 2D Janus crystal synthesis. Another route of growth could be Janus layer formation from exfoliated monolayers. This would enable one to start with exfoliated sheets from vdW crystals—instead of extensive CVD parameter development for exotic material systems—and create new classes of Janus layers by surface replacement mechanisms. While this process is not scalable, it will enable researchers to probe novel quantum phenomena in microscales and identify promising 2D Janus candidates for a variety of

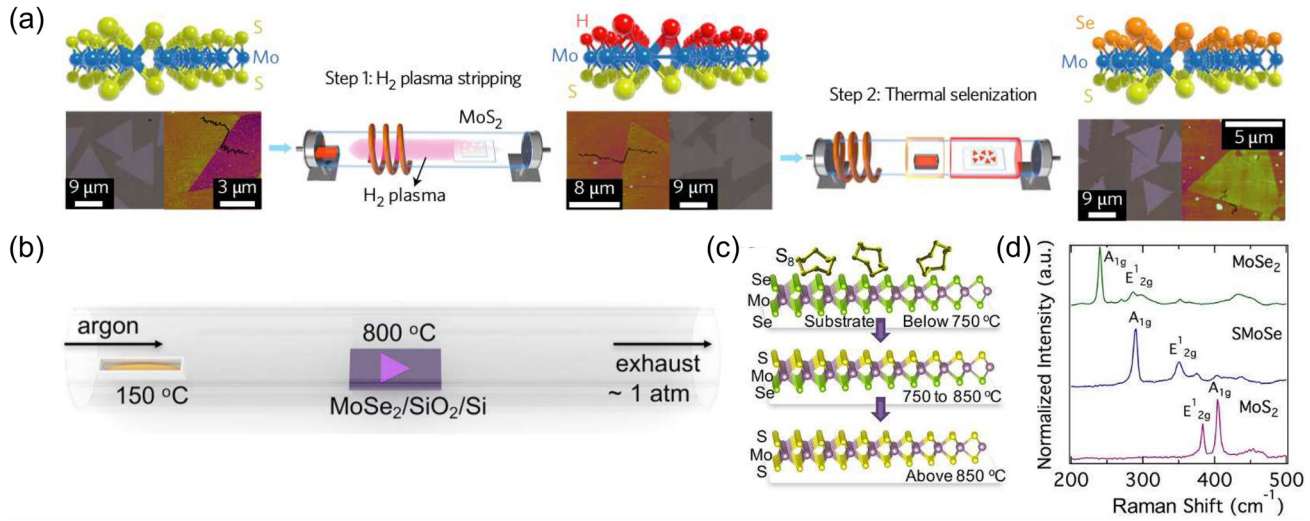

FIG. 7. Two main techniques emerged for the fabrication of 2D Janus MoSSe. (a) The first one strip off the top S layer, hydrogenize, and eventually selenide the surface.[40] Reprinted with permission from Lu *et al.*, Nat. Nanotechnol. **12**(8), 744 (2017). Copyright 2017 Springer Nature. (b) The second technique removes the top layer by thermal annealing and decorates the top surface with different types of chalcogens.[39] Reprinted with permission from Zhang *et al.*, ACS Nano **11**(8), 8192–8198 (2017). Copyright 2017 American Chemical Society.

applications. Finally, solution-process-based techniques are needed to transform classical TMDs into Janus layers, which will enable room temperature processing that is required in the industry.

C. Other theoretically predicted Janus TMDs layers

Following the experimental realization of Janus single-layer MoSSe and the theoretical investigation of out-of-plane piezoelectricity in the Janus family, a large number of Janus TMD single-layers were predicted theoretically. Shi *et al.* studied the structural, electronic, and mechanical properties of Janus single-layer MXY (M = Ti, Zr, Hf, V, Nb, Ta, Cr, Mo, or W and X/Y = S, Se, or Te) structures.[74] It was first shown that except for the VXY, TiSSe, and TiSTe single-layers, all structures display dynamical stability in the 1H phase revealed by the real phonon band dispersions through the whole Brillouin zone. The reason for the dynamical instability of the mentioned single-layers of V- and Ti-based Janus structures can be due to the existing charge density wave phase in V- and Ti-based TMDs in their bare structures. As shown in Fig. 8, the mechanical properties of all structures were investigated in terms of their elastic constants, and they were compared through the atomic masses and radius. It was also shown that Janus single-layers of Hf-, Zr-, and Ti-dichalcogenides exhibit metallic behavior in contrast to their non-polar symmetric single-layer forms. Also, it was revealed that single-layer VSSe has a giant in-plane piezoelectric polarization and exhibits an intrinsic ferroelasticity. Moreover, it was shown that the in-plane piezoelectricity in Janus VSSe could be tuned up to $\sim 3.3 \times 10^{-10}$ C/m as it is subjected to uniaxial in-plane strain. Remarkably, an ultrahigh reversible strain (up to 73%) was demonstrated in the ferroelasticity of Janus VSSe that is much higher than that reported for other 2D materials.

Inspired by the synthesis of VS_2 and demonstration of ferromagnetic order in 2D,[62] Zhang *et al.* predicted that Janus single-layer VSSe exhibits a highly stable room-temperature ferromagnetism and a large valley polarization arising from the broken space- and time-reversal symmetries.[66] Although theoretical investigations on the stability of Janus TMDs single-layers were made by considering only their 1H phase, the Te-based Janus structures may also exhibit dynamical stability in their distorted phase (1T′) since $MoTe_2$ and WTe_2 were reported to crystallize in 1T′ phase.[75,76] Experimental studies reported structural phase transitions from 1H to 1T′ via electrostatic charge injection in Te-based TMDs.[77] Wang *et al.* reported such a 1H to 1T′ phase transition upon electron doping in Janus single-layers of MoSSe and MoSTe using first-principles calculations.[78] It was predicted that the critical value of electron doping for such a phase transition depends on the type of the chalcogenide atoms and that the electron amount decreases from S to Te. Notably, such a structural phase transition can be easily achieved in Janus MoSTe via small amount of electron doping. On the other hand, Tang *et al.* predicted that Janus single-layer MoSSe could also crystallize in dynamically stable IT′ phase which exhibits distinctive properties as compared to its 1H phase.[79] Similar to the electron doping strategy, it was reported that the energy barrier (1.10 eV) between 1H and 1T′ phases of Janus MoSSe can be overcome via alkali metal adsorption which is a feasible experimental approach. Notably, due to the almost linear dispersion of the band states, an ultrahigh electron (hole) mobility up to 1.21×10^5 (7.24×10^4) $cm^2/(V\,s)$ was calculated for the 1T′ phase. Recently, the vibrational and piezoelectric properties of Janus MoSTe phases were calculated.[80] It was shown that the dynamically stable IH and 1T′ phases of Janus MoSTe exhibit distinctive vibrational properties in terms of their Raman spectra. In addition, the noncentral symmetric 1T′-MoSTe was shown to possess large piezoelectric coefficients.

D. 2D Janus vdW superlattices and interfaces

The quantum confinement of electrons at atomic scale and the presence of interlayer coupling in van der Waals layered materials

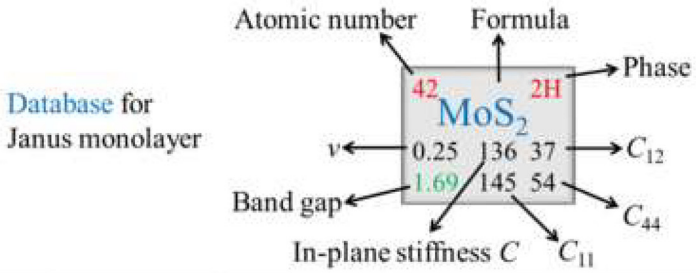

22 1T TiS_2 0.23 79 20 0.01 84 32	22 1T TiSSe 0.20 66 14 mtal 69 27	22 1T $TiSe_2$ 0.21 70 15 mtal 73 29	22 1T TiSTe 0.39 44 20 mtal 52 16	22 1T TiSeTe 0.31 45 15 mtal 50 17	22 1T $TiTe_2$ 0.26 56 15 mtal 60 22
40 1T ZrS_2 0.21 78 17 0.85 82 32	40 1T ZrSSe 0.25 62 17 0.43 67 25	40 1T $ZrSe_2$ 0.22 60 14 0.19 63 25	40 1T ZrSTe 0.27 49 14 mtal 53 19	40 1T ZrSeTe 0.28 46 14 mtal 50 18	40 1T $ZrTe_2$ 0.24 36 10 mtal 38 14
72 1T HfS_2 0.22 72 17 0.92 76 30	72 1T HfSSe 0.24 68 17 0.45 72 27	72 1T $HfSe_2$ 0.23 60 15 0.31 64 24	72 1T HfSTe 0.27 53 15 mtal 57 21	72 1T HfSeTe 0.26 51 14 mtal 55 20	72 1T $HfTe_2$ 0.21 50 11 mtal 52 20
23 1T VS_2 0.53 41 30 mtal 57 13	23 1T VSSe 0.42 51 26 mtal 62 18	23 1T VSe_2 0.44 60 37 mtal 75 21	23 1T VSTe 0.56 30 24 mtal 44 10	23 1T VSeTe 0.53 32 24 mtal 45 10	23 1T VTe_2 0.42 49 25 mtal 60 17
41 2H NbS_2 0.38 88 40 mtal 103 32	41 2H NbSSe 0.35 80 32 mtal 92 30	41 2H $NbSe_2$ 0.37 64 27 mtal 74 23	41 2H NbSTe 0.43 50 26 mtal 62 18	41 2H NbSeTe 0.31 70 24 mtal 77 27	41 2H $NbTe_2$ 0.34 62 24 0.20 71 23
73 2H TaS_2 0.39 82 38 mtal 97 30	73 2H TaSSe 0.42 75 38 mtal 92 27	73 2H $TaSe_2$ 0.35 72 29 mtal 82 27	73 2H TaSTe 0.37 72 31 mtal 84 26	73 2H TaSeTe 0.32 76 27 mtal 85 29	73 2H $TaTe_2$ 0.32 49 17 mtal 54 18
24 1T CrS_2 0.41 58 29 mtal 70 21	24 1T CrSSe 0.31 42 15 mtal 47 16	24 1T $CrSe_2$ 0.58 36 33 mtal 55 11	24 1T CrSTe 0.69 22 30 mtal 43 7	24 1T CrSeTe 0.45 35 20 mtal 44 12	24 1T $CrTe_2$ 0.22 65 12 mtal 67 30
42 2H MoS_2 0.25 136 37 1.69 145 54	42 2H MoSSe 0.24 106 27 1.55 112 43	42 2H $MoSe_2$ 0.29 106 33 1.45 116 41	42 2H MoSTe 0.24 115 30 0.94 124 47	42 2H MoSeTe 0.23 117 28 1.34 122 47	42 2H $MoTe_2$ 0.28 84 25 1.18 91 32
74 2H WS_2 0.21 158 34 1.91 165 65	74 2H WSSe 0.20 143 30 1.85 149 60	74 2H WSe_2 0.26 102 29 1.73 110 40	74 2H WSTe 0.17 139 25 1.31 143 59	74 2H WSeTe 0.17 146 25 1.54 150 62	74 1T' WTe_2 0.34 98 37 0.20 110 36

FIG. 8. The list of predicted 2D Janus TMDs, their phases, bandgaps, and in-plane stiffness.[74] Reprinted with permission from Shi *et al.*, J. Phys. **30**(21), 215301 (2018). Copyright 2018 IOP Publishing, Ltd.

provide researchers with an opportunity to tune their electronic and optical properties through stacking engineering.[81] While the properties of many 2D materials are sensitive to the sample thickness such as MoS_2 (which exhibits an indirect-to-direct bandgap crossover as it is thinned down to the one-layer limit),[51] ReS_2 was observed to be a robust direct bandgap semiconductor regardless of the number of layers.[82]

Similar to the van der Waals heterostructures constructed from 2D materials, those formed by two Janus single-layers or by Janus and bare single-layer materials have also become the focus of interest due to possible interface variations caused by the asymmetry and the permanent dipole within each layer. Li *et al.* studied the electronic and optical properties of both vertical and lateral MoSSe/WSSe heterostructures, and it was revealed that both types possess type-II band alignment which is desirable for energy conversion because of the induced spatially indirect excitons [Figs. 9(a) and 9(b)].[55] Yin *et al.* investigated the layer number-dependent properties of Janus MoSSe.[81] It was shown that the MoSSe layers prefer to interact in SMoSe/SMoSe sequence in their bilayer form, which enhances the induced out-of-plane dipole moment. In addition, the bandgap and the charge carrier mobilities were shown to be effectively modified via stacking type and the layer number. Particularly, the electronic dispersions were shown to vary from indirect to direct, and the bandgap can be controlled between 0.81 and 1.45 eV via stacking order. Moreover, Riis-Jensen *et al.* reported that the intrinsic dipole moment leads to the formation of a built-in electric field as the layer number increases.[72] It was shown that the electric field induces a staggered (type-II) band alignment throughout the structure, and at a critical thickness of 3–4 layers, the conduction band minimum of the upper-most layer was found to meet the valence band maximum of the lower-most layer triggering an electron transfer between the outermost monolayers [see Fig. 9(b)]. The charge density on the outermost surfaces of the created p-n junction was also calculated, and it was shown that the charge density can be tuned from 5×10^{12} (in 5L-MoSSe) to 2×10^{13} e/cm^2 (in 17L-MoSSe). The results are particularly exciting for charge separation in solar cells or tuning of band alignment at the interface between two different semiconductors. Another area of excitement will be excitonics, where interlayer excitons and formation of exciton complexes through various thermalization pathways enabled by the permanent dipole or colossal polarization fields are valuable.

a. Interfaces with other materials. On the other hand, Yu *et al.* investigated the interfacial contact properties of graphene/MoSSe heterostructure and reported that the formed n-type Schottky contact have a Schottky barrier height of 0.07 eV, and it is tunable down to the Ohmic contact via application of external electric field (>0.4 V/Å) and in-plane biaxial strain (>8%).[83] Similarly, Jing *et al.* studied the interfacial properties of heterostructures constructed by Janus MSSe (M = Mo or W) and Hf_2NT_2 (T = F, O, or OH) single-layers.[84] Particularly, it was shown that using the S or Se face MSSe in contact with Hf_2NT_2 layer significantly affects the Schottky barrier height. Furthermore, the choice of F atom on the surface of Hf_2N in contact with S-terminated surfaces of MoSSe or WSSe was shown to create Schottky barrier-free contact for electron injection. As revealed by those studies, in constructed vertical heterostructures of Janus single-layers, the atomic termination of the interface has significant effects on the properties of the system. Our group investigated the single-layer Janus structures of Pt-dichalcogenides and their possible vertical heterostructures.[85] It was also reported that the replacement of surface atoms with smaller chalcogen atoms is favorable for the formation of Janus XPtY (X ≠ Y = S, Se, or Te). Also, it was shown that vertical heterostructures constructed either by XPtY/XPtY or XPtY/Pt_2X provide a wide range of opportunities for possible applications due to the creation of type I, II, and III band alignments.

IV. TUNABLE QUANTUM PROPERTIES

A. Strain-Rashba Relation

The in-plane strain directly influences the net electric field acting on metal atoms within the Janus lattice, and thus also affects the Rashba spin splitting.[59] Li *et al.* showed that changing the interlayer distance causes variation of the Rashba effect which arises from the competition between the intralayer and interlayer electric fields.[54] The contrast of Rashba parameters α_R at Γ high symmetry point as a function of interlayer distance was simulated. It was shown that in the case

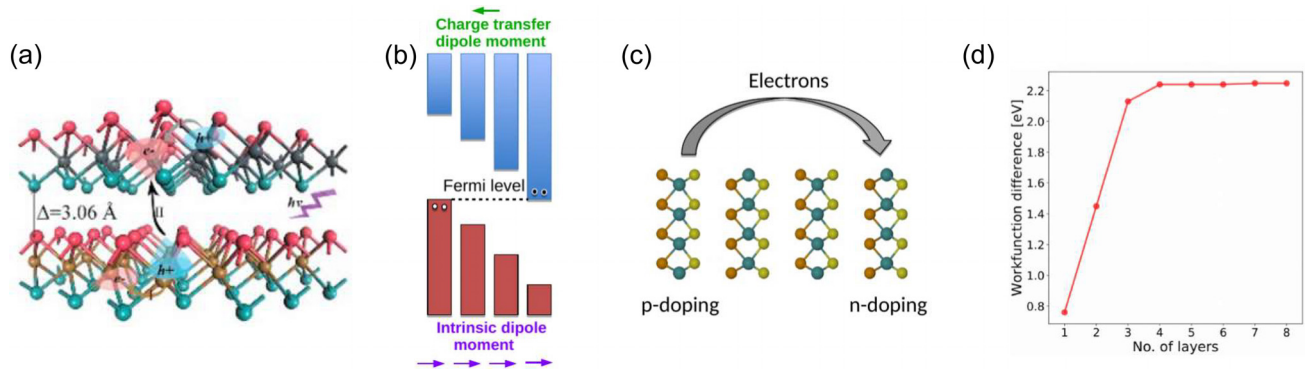

FIG. 9. (a) Formation of interlayer excitons in 2D Janus MoSSe/WSSe vdW junctions in the presence of strong polarization field.[55] Reprinted with permission from Li *et al.*, J. Phys. Chem. Lett. **8**(23), 5959–5965 (2017). Copyright 2017 American Chemical Society. (b) and (c) Formation of type-II homojunction in 2D Janus TMDs and efficient photo-excited hole and electron separation.[72] (d) The work function difference between the top and the bottom layers show strong variation with respect to the number of layers used in vdW homojunction formation.[72] Reprinted with permission from Riis-Jensen *et al.*, J. Phys. Chem. C **122**(43), 24520–24526 (2018). Copyright 2018 American Chemical Society.

of increased interlayer distance from equilibrium, a decreased overlap between p_z orbitals in S/Se leads to an enhanced net vertical electric field, triggering significant large α_R values. The Rashba effect, however, disappeared as the interlayer distance was reduced (Fig. 10).

When compressive strain is applied on AA-stacked MoSSe layers, α_R as large as 1.28 eV Å can be obtained. In contrast, due to tensile strain, a decrease in the out-of-plane orbital overlap resulted in a net vertical reduction of the electric fields experienced by Mo atoms, resulting in the absence of the Rashba effect. It is consequently decisive that an in-plane strain provides an effective way to tune the Rashba effect in monolayer MoSSe and stacking structures. Subsequently, due to auxiliary strain, the in-plane electric field is also tuned, causing valley splitting at band edges. This was confirmed by the VB splitting ($\lambda k\nu$) at the K point when the strain was changed. Considering the large values of Rashba coefficients, together with the ability to tune these values further to even higher values by strain, Janus materials offer different directions in spin-FETs and spintronics.

B. Electronic effects

The strain phenomena in Janus single-layers were further extended to many different TMDs Janus structures. By considering 1H-phase of single-layer MXY (M = Mo or W, and X ≠ Y = S, Se, or Te), Liu *et al.* investigated their in-plane biaxial strain-dependent electronic properties.[86] Structurally, it was shown that the single-layer Janus MXY structures maintain their dynamical stability even at large compressive (12%) and tensile (14%) biaxial strains. Moreover, it was shown that regardless of the type of the chalcogen and transition metal atom, all Janus MXY structures exhibit semiconducting to metallic transition with an increase in the biaxial strain. Like the distorted phase of TMDs single-layers, the square phase (1S) of Janus MXY (M = Mo or W, and X ≠ Y = S, Se, or Te) was studied by Zhang *et al.* and was reported to possess dynamical stability.[87] The bare 1S-MXY single-layers were found to be semiconductors with energy bandgaps ranging from 30 to 165 meV. Besides, it was revealed that 1S-MoSeTe, 1S-WSSe, and 1S-WSeTe undergo a semiconductor-metal transition upon application of compressive strain in the range 3%–6%. Moreover, single-layer 1S-WSTe was shown to exhibit strain-dependent spin–orbit splitting with the most significant value of 129 meV under 3% of compressive strain.

The experimental realization of Janus MoSSe has opened up the possibility for the synthesis of other single-layer Janus structures of TMDs. Janus single-layer of WX_2 (X = S, Se, or Te) also has such potential due to its similar structure as Mo-dichalcogenides. Kandemir *et al.* investigated the electronic and vibrational properties of single-layer and bilayer Janus WSSe.[89] It was revealed that Janus WSSe is a direct bandgap semiconductor and its Raman spectrum exhibits additional phonon modes which arise due to the broken out-of-plane symmetry. In addition, it was shown that for three possible atomic arrangements in the interface of bilayer WSSe (S–Se, S–S, and Se–Se), Raman spectra possess a wide variety of features, which are useful for distinguishing the stacking type (see Fig. 11). In another study, Zhou *et al.* studied the structural stability and electronic properties of few-layer WSSe and reported that the atomic order of Se–S–Se–S in bilayer WSSe has a significant layer splitting because of the net total dipole moment which can be useful for solar cell applications.[88] The electronic structures and spin splitting were reported to be sensitive to the chalcogen atomic-layer order and the interlayer distance in a few-layer Janus WSSe.

C. Effect of atomic adsorption

It was demonstrated by experiments and predicted theoretically that 2D materials are quite suitable for tuning their properties by atomic and molecular adsorptions, electrostatic gating, and straining.[90] Janus single-layer materials were also considered to be suitable candidates for such tuning due to asymmetric surfaces, which may enable the emergence of combined properties under external effects. Tao *et al.* studied the effect of transition metal atom adsorption on single-layer Janus MoSSe structure.[91] The adsorption from Se-side results in enhanced dipole moment, regardless of the binding site of the adatom. In contrast, for adsorption of transition metals from the S-side, the dipole moments are weakened or even reversed depending on the type of adsorbed atom. In another study, Peng *et al.* investigated the valleytronic properties of single-layer Janus MoSSe and reported that its direct bandgap nature at the K point accommodates coupled spin and valley physics as a result of the strong spin–orbit coupling (SOC) and the broken out-of-plane symmetry. It was found that upon magnetic atom doping, i.e., Cr/V, valley polarization can be achieved, which is also strain-tunable. Effect of magnetic dopants on the valley polarization in single-layer Janus MoSSe was reported, and it was shown that the long-sought valley polarization could be achieved via Cr/V magnetic doping which is essential for valleytronics.[92]

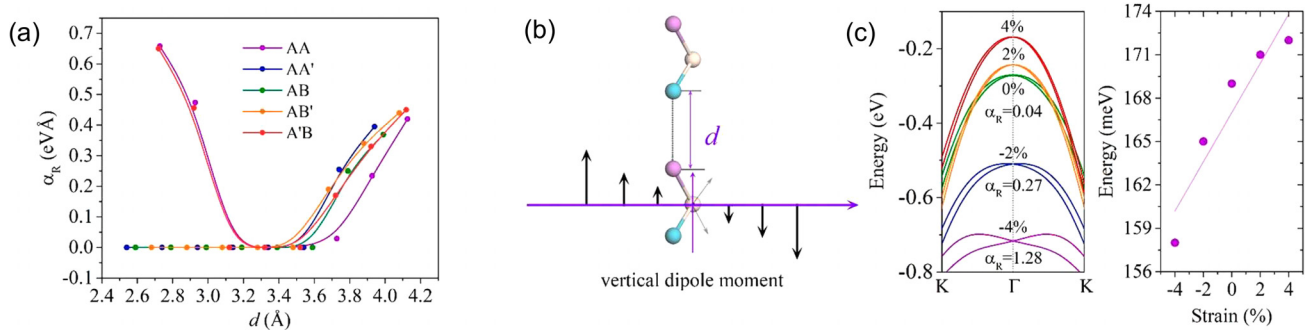

FIG. 10. Tunable (a) Rashba splitting parameters, (b) vertical polarization strength acting on metal atom via stacking distance, and (c) Rashba energies via biaxial strain for AA stacked MoSSe.[54] Reprinted with permission from Li *et al.*, J. Phys. Chem. Lett. **10**(3), 559–565 (2019). Copyright 2019 American Chemical Society.

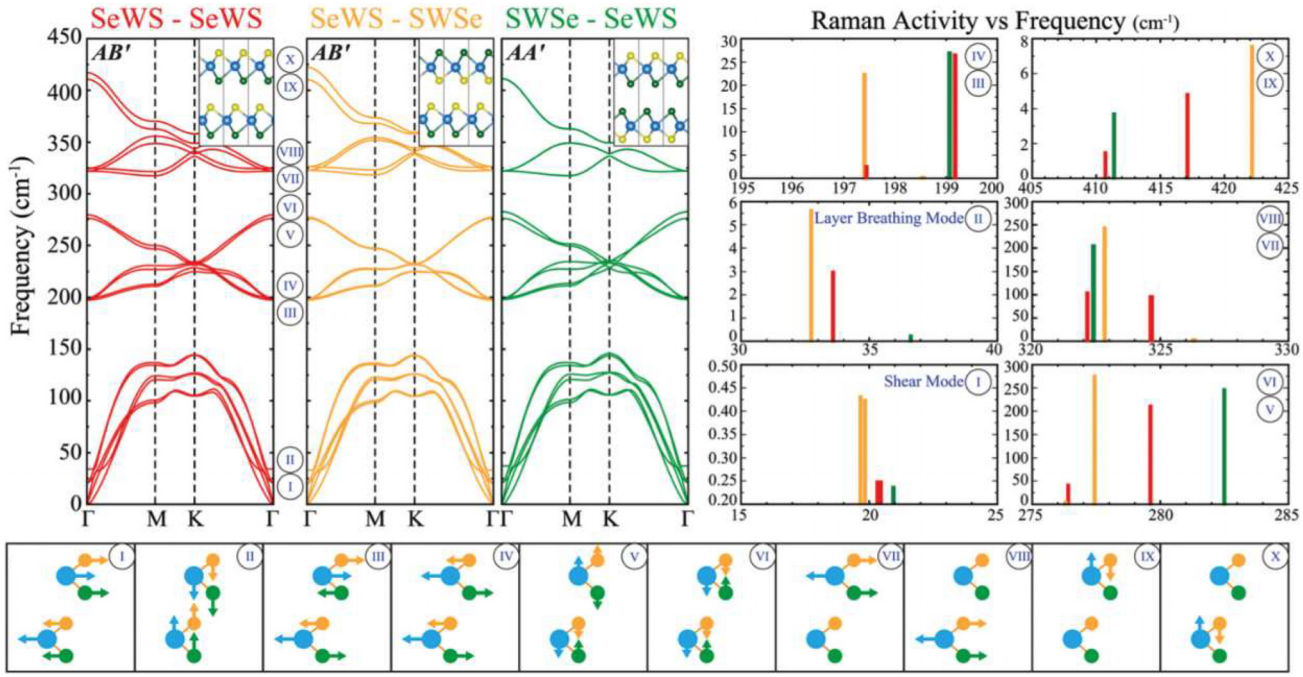

FIG. 11. Calculated phonon dispersions and Raman active modes for SeWS Janus material with different stacking orders.[89] Reprinted with permission from Kandemir *et al.*, Phys. Chem. Chem. Phys. **20**(25), 17380–17386 (2018). Copyright 2018 Royal Society of Chemistry.

V. OTHER 2D JANUS LAYERS

A. Post-transition-metal chalcogenides: M_2XY (M = Ga or In, X = Y = S, Se, or Te)

Post-transition-metal chalcogenides (PTMCs) are essential examples of vdW layered materials having the chemical formula MX where M stands for post-transition-metal and X for the chalcogenide atom. Over the last five years, single-layers of GaS and GaSe were successfully added to the 2D library[93–95] and very recently, their cousin, InSe, was announced to be a potential semiconductor for superfast electronic devices due to its high electron mobility at room temperature.[96]

Considering their attractive properties and application areas in photovoltaics and catalysis, Guo *et al.*[97] designed possible Janus single-layers of group-III monochalcogenides (including Ga_2SSe, Ga_2STe, Ga_2SeTe, In_2SSe, In_2STe, In_2SeTe, $GaInS_2$, $GaInSe_2$, and $GaInTe_2$) and it was shown that all of the Janus structures possess thermodynamical and dynamical stabilities. Also, electronic band dispersion calculations revealed that the bandgap of the Janus structures lies in the range of 0.89 and 2.03 eV and Ga_2STe, Ga_2SeTe, In_2STe, and In_2SeTe were found to exhibit direct bandgap behavior. This indirect to direct gap crossover is particularly exciting, and more advanced quantum simulations are needed to understand the excitonic and potential valleytronic properties.

Moreover, the piezoelectric coefficients of Janus group-III monochalcogenides were found to be enhanced up to 8.47 pm/V, which is over four times the maximum value of the classical PTMCs structures. The out-of-plane polarization was shown to result in an additional out-of-plane piezoelectric coefficient ranging between 0.07 and 0.46 pm/V orders of magnitude stronger than that of TMDs Janus structures (see Fig. 12).

In another study, the strain-dependent electronic properties of In_2SSe Janus single-layers were studied, and it was shown that Janus In_2SSe possesses a direct bandgap.[98] This is in stark contrast to other classical In-based M_2X_3 systems, and more experimental studies are needed to confirm this finding. Besides, it was shown that excessive uniaxial and biaxial strain ranges (±2%), Janus In_2SSe behaves as a robust direct bandgap semiconductor even when put on substrates, which may be quite crucial for applications in optoelectronic devices.

Furthermore, Bai *et al.* predicted potential applications of single-layer Janus PTMCs as photocatalysts.[99] It was shown that the band edge positions of the Janus PTMCs are suitable for photocatalytic water splitting except for the single-layer Ga_2STe, whose valence band edge is higher than the oxidation potential. Also, the direct bandgap nature of Ga_2SeTe, In_2STe, and In_2SeTe makes them potential candidates for application in the field of photocatalysis because of their high absorption coefficient and their highly efficient electron-hole pair generation (Fig. 13). Other than these attractive electronic properties, it remains unknown how the permanent dipole in 2D Janus chalcogenides influences the overall catalytic activity or if selective catalysis (driven by the polarization field) can be achieved.

VI. SUMMARY AND OVERVIEW

In this review article, we discussed the recent progress in 2D Janus materials with emphasis on emergent quantum phenomena arising from broken mirror symmetry and colossal polarization (vertical electric field) in these unique classes of materials. We have provided an update of the fundamental electronic, magnetic, optical, and piezoelectric properties of these material systems. While doing so, we have put them in a historical context concerning 0D and 1D Janus

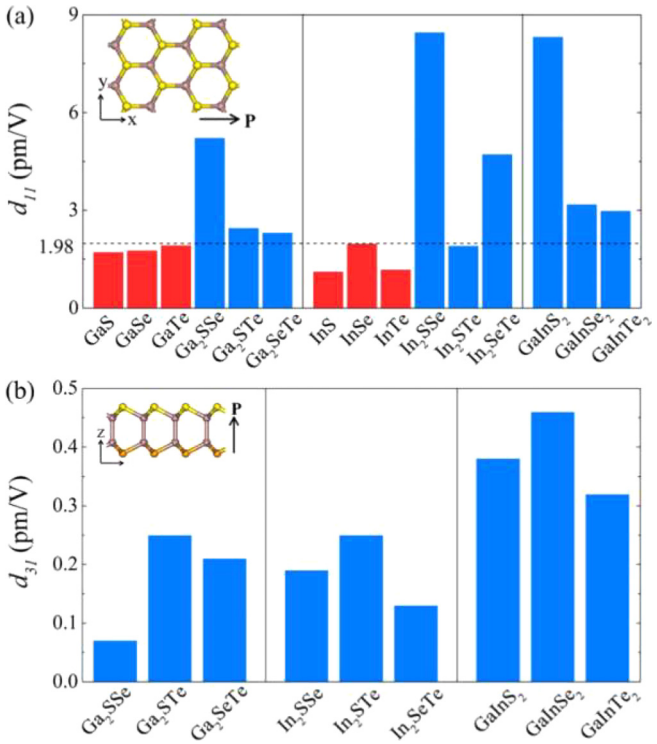

FIG. 12. Extraordinary piezoelectric coefficients predicted for a variety of Ga- and In- based 2D Janus layers.[97] Reprinted with permission from Guo *et al.*, Appl. Phys. Lett. **110**(16), 163102 (2017). Copyright 2017 AIP Publishing.

materials. 2D Janus materials included graphene-based, TMDs, PTMCs, and other types of Janus crystals.

In the big picture, the future of 2D Janus layers is bright. They offer rather unique properties that lead to many important application areas in quantum sciences, energy conversion technologies, and spintronics. Superlattices of 2D Janus layers offer efficient ways to separate photoexcited changes and even provide novel approaches for band-alignment engineering. These attributes suggest that their superlattices are likely to make an impact in energy conversion—the built-in polarization field in 2D Janus chalcogenides is likely to create ways for selective catalysis and spin-dependent chemistry. Unique layer to layer polarization field interactions have been theoretically shown to generate rather powerful piezoelectric parameters. While this is yet to be experimentally demonstrated, Janus layers will likely make meaningful contributions to the piezoelectrics field. Other than these straightforward directions, we anticipate that their quantum properties arising from exotic many-body interaction in the presence of self-driven polarization fields will unlock novel properties and applications that are not possible with other material systems. Examples include magnetic knots (skyrmions) engineering, spintronics by 2D magnetic ordering, quantum opto-spintronics, or valleytronics by dipolar excitons in Janus layers, and traditional spintronic/qubit operations enabled by giant Rashba splitting. However, at the time of writing this review article, the majority of the work is still theory driven. While a wealth of quantum and physical effects have been predicted, the experimental results are severely lacking, likely due to difficulties in sample preparation. We anticipate essential progress in the fundamental understanding of these materials once the synthesis techniques become more accessible and more reproducible, and the characterization teams start gaining access to these material systems.

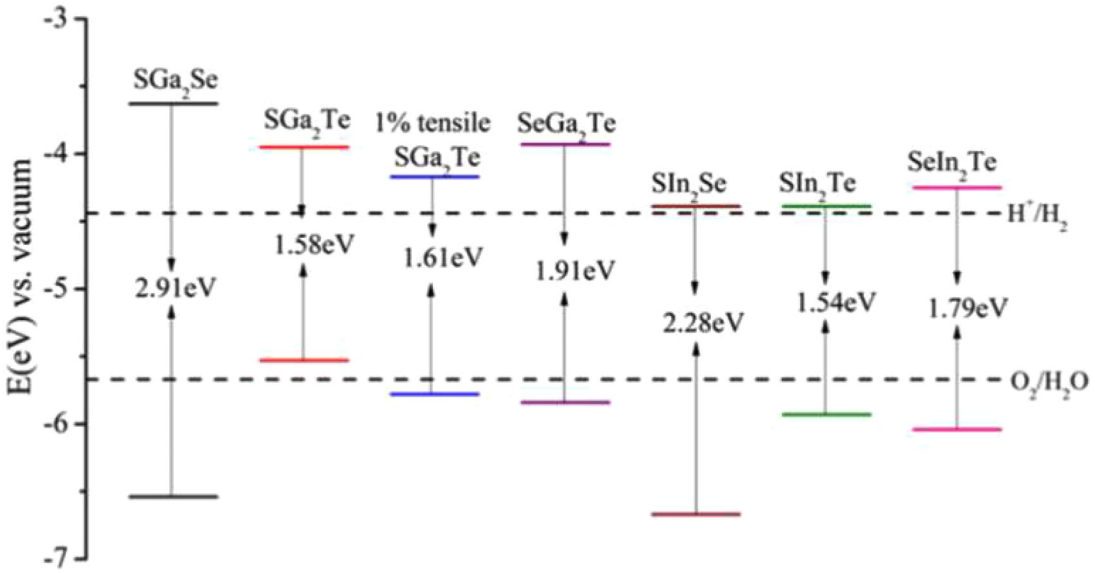

FIG. 13. The potential of 2D Janus PTMCs toward catalysis and photovoltaics. The position of valence band (VB) and conduction band (CB) edges is shown.[99] Reprinted with permission from Bai *et al.*, Appl. Surf. Sci. **478**, 522–531 (2019). Copyright 2019 Elsevier.

AUTHOR'S CONTRIBUTIONS

M.Y. and Y.Q. contributed equally to this work.

ACKNOWLEDGMENTS

S.T. acknowledges support from NSF Contract Nos. DMR 1552220, DMR 1904716, and NSF CMMI 1933214. H.S. acknowledges financial support from the Scientific and Technological Research Council of Turkey (TUBITAK) under Project No. 117F095. H.S. acknowledges support from the Turkish Academy of Sciences under the GEBIP program. M.Y. is supported by the Flemish Science Foundation (FWO-Vl) through a postdoctoral fellowship. Part of this work was supported by the FLAG-ERA project TRANS2D-TMD.

REFERENCES

[1]C. Casagrande, P. Fabre, E. Raphael, and M. Veyssié, "'Janus beads': Realization and behaviour at water/oil interfaces," Europhys. Lett. **9**(3), 251 (1989).
[2]A. Kharazmi and N. V. Priezjev, "Diffusion of a Janus nanoparticle in an explicit solvent: A molecular dynamics simulation study," J. Chem. Phys. **142**(23), 234503 (2015).
[3]M. Danial, C. M.-N. Tran, P. G. Young, S. Perrier, and K. A. Jolliffe, "Janus cyclic peptide–polymer nanotubes," Nat. Commun. **4**, 2780 (2013).
[4]L. Zhang, J. Yu, M. Yang, Q. Xie, H. Peng, and Z. Liu, "Janus graphene from asymmetric two-dimensional chemistry," Nat. Commun. **4**, 1443 (2013).
[5]Q. Peng, A. K. Dearden, X.-J. Chen, C. Huang, X. Wen, and S. De, "Peculiar pressure effect on Poisson ratio of graphene as a strain damper," Nanoscale **7**(22), 9975–9979 (2015).
[6]J. Du and R. K. O'Reilly, "Anisotropic particles with patchy, multicompartment and Janus architectures: Preparation and application," Chem. Soc. Rev. **40**(5), 2402–2416 (2011).
[7]A. Walther and A. H. Muller, "Janus particles: Synthesis, self-assembly, physical properties, and applications," Chem. Rev. **113**(7), 5194–5261 (2013).
[8]A. Kumar, B. J. Park, F. Tu, and D. Lee, "Amphiphilic Janus particles at fluid interfaces," Soft Matter **9**(29), 6604–6617 (2013).
[9]J. He, M. J. Hourwitz, Y. Liu, M. T. Perez, and Z. Nie, "One-pot facile synthesis of Janus particles with tailored shape and functionality," Chem. Commun. **47**(46), 12450–12452 (2011).
[10]C. Salvador-Morales, P. M. Valencia, W. Gao, R. Karnik, and O. C. Farokhzad, "Spontaneous formation of heterogeneous patches on polymer–lipid core–shell particle surfaces during self-assembly," Small **9**(4), 511–517 (2013).
[11]Y. Zhang, K. Huang, J. Lin, and P. Huang, "Janus nanoparticles in cancer diagnosis, therapy and theranostics," Biomater. Sci. **7**(4), 1262–1275 (2019).
[12]A. Perro, F. Meunier, V. Schmitt, and S. Ravaine, "Production of large quantities of "Janus" nanoparticles using wax-in-water emulsions," Colloids Surf. A **332**(1), 57–62 (2009).
[13]R. F. Shepherd, J. C. Conrad, S. K. Rhodes, D. R. Link, M. Marquez, D. A. Weitz, and J. A. Lewis, "Microfluidic assembly of homogeneous and Janus colloid-filled hydrogel granules," Langmuir **22**(21), 8618–8622 (2006).
[14]J.-W. Kim, R. J. Larsen, and D. A. Weitz, "Synthesis of nonspherical colloidal particles with anisotropic properties," J. Am. Chem. Soc. **128**(44), 14374–14377 (2006).
[15]T. Isojima, M. Lattuada, J. B. Vander Sande, and T. A. Hatton, "Reversible clustering of pH-and temperature-responsive Janus magnetic nanoparticles," ACS Nano **2**(9), 1799–1806 (2008).
[16]A. Walther, M. Drechsler, S. Rosenfeldt, L. Harnau, M. Ballauff, V. Abetz, and A. H. Müller, "Self-assembly of Janus cylinders into hierarchical superstructures," J. Am. Chem. Soc. **131**(13), 4720–4728 (2009).
[17]A. Walther, M. Drechsler, and A. H. Müller, "Structures of amphiphilic Janus discs in aqueous media," Soft Matter **5**(2), 385–390 (2009).
[18]A. Walther and A. H. Müller, "Janus particles," Soft Matter **4**(4), 663–668 (2008).
[19]A. Walther, K. Matussek, and A. H. Muller, "Engineering nanostructured polymer blends with controlled nanoparticle location using Janus particles," ACS Nano **2**(6), 1167–1178 (2008).
[20]L. Y. Wu, B. M. Ross, S. Hong, and L. P. Lee, "Bioinspired nanocorals with decoupled cellular targeting and sensing functionality," Small **6**(4), 503–507 (2010).
[21]S.-H. Hu and X. Gao, "Nanocomposites with spatially separated functionalities for combined imaging and magnetolytic therapy," J. Am. Chem. Soc. **132**(21), 7234–7237 (2010).
[22]J. R. Howse, R. A. Jones, A. J. Ryan, T. Gough, R. Vafabakhsh, and R. Golestanian, "Self-motile colloidal particles: From directed propulsion to random walk," Phys. Rev. Lett. **99**(4), 048102 (2007).
[23]Y. Lu, H. Xiong, X. Jiang, Y. Xia, M. Prentiss, and G. M. Whitesides, "Asymmetric dimers can be formed by dewetting half-shells of gold deposited on the surfaces of spherical oxide colloids," J. Am. Chem. Soc. **125**(42), 12724–12725 (2003).
[24]H. Y. Koo, D. K. Yi, S. J. Yoo, and D. Y. Kim, "A snowman-like array of colloidal dimers for antireflecting surfaces," Adv. Mater. **16**(3), 274–277 (2004).
[25]Z. Li, D. Lee, M. F. Rubner, and R. E. Cohen, "Layer-by-layer assembled Janus microcapsules," Macromolecules **38**(19), 7876–7879 (2005).
[26]D. Dendukuri and P. S. Doyle, "The synthesis and assembly of polymeric microparticles using microfluidics," Adv. Mater. **21**(41), 4071–4086 (2009).
[27]K. S. Novoselov, A. K. Geim, S. V. Morozov, D. Jiang, Y. Zhang, S. V. Dubonos, I. V. Grigorieva, and A. A. Firsov, "Electric field effect in atomically thin carbon films," Science **306**(5696), 666–669 (2004).
[28]A. K. Geim and I. V. Grigorieva, "Van der Waals heterostructures," Nature **499**(7459), 419 (2013).
[29]L. Britnell, R. Gorbachev, R. Jalil, B. Belle, F. Schedin, A. Mishchenko, T. Georgiou, M. Katsnelson, L. Eaves, and S. Morozov, "Field-effect tunneling transistor based on vertical graphene heterostructures," Science **335**(6071), 947–950 (2012).
[30]H. Fang, C. Battaglia, C. Carraro, S. Nemsak, B. Ozdol, J. S. Kang, H. A. Bechtel, S. B. Desai, F. Kronast, and A. A. Unal, "Strong interlayer coupling in van der Waals heterostructures built from single-layer chalcogenides," Proc. Natl. Acad. Sci. **111**(17), 6198–6202 (2014).
[31]C.-H. Lee, G.-H. Lee, A. M. Van Der Zande, W. Chen, Y. Li, M. Han, X. Cui, G. Arefe, C. Nuckolls, and T. F. Heinz, "Atomically thin p–n junctions with van der Waals heterointerfaces," Nat. Nanotechnol. **9**(9), 676 (2014).
[32]B. Hunt, J. Sanchez-Yamagishi, A. Young, M. Yankowitz, B. J. LeRoy, K. Watanabe, T. Taniguchi, P. Moon, M. Koshino, and P. Jarillo-Herrero, "Massive Dirac fermions and Hofstadter butterfly in a van der Waals heterostructure," Science **340**(6139), 1427–1430 (2013).
[33]X. Hong, J. Kim, S.-F. Shi, Y. Zhang, C. Jin, Y. Sun, S. Tongay, J. Wu, Y. Zhang, and F. Wang, "Ultrafast charge transfer in atomically thin MoS_2/WS_2 heterostructures," Nat. Nanotechnol. **9**(9), 682 (2014).
[34]A. C. Ferrari, F. Bonaccorso, V. Fal'Ko, K. S. Novoselov, S. Roche, P. Bøggild, S. Borini, F. H. Koppens, V. Palermo, and N. Pugno, "Science and technology roadmap for graphene, related two-dimensional crystals, and hybrid systems," Nanoscale **7**(11), 4598–4810 (2015).
[35]C. Tan and H. Zhang, "Two-dimensional transition metal dichalcogenide nanosheet-based composites," Chem. Soc. Rev. **44**(9), 2713–2731 (2015).
[36]J. S. Ross, P. Klement, A. M. Jones, N. J. Ghimire, J. Yan, D. Mandrus, T. Taniguchi, K. Watanabe, K. Kitamura, and W. Yao, "Electrically tunable excitonic light-emitting diodes based on monolayer WSe_2 p–n junctions," Nat. Nanotechnol. **9**(4), 268 (2014).
[37]M. M. Furchi, A. Pospischil, F. Libisch, J. Burgdörfer, and T. Mueller, "Photovoltaic effect in an electrically tunable van der Waals heterojunction," Nano Lett. **14**(8), 4785–4791 (2014).
[38]E. Calman, C. Dorow, M. Fogler, L. Butov, S. Hu, A. Mishchenko, and A. Geim, "Control of excitons in multi-layer van der Waals heterostructures," Appl. Phys. Lett. **108**(10), 101901 (2016).
[39]J. Zhang, S. Jia, I. Kholmanov, L. Dong, D. Er, W. Chen, H. Guo, Z. Jin, V. B. Shenoy, and L. Shi, "Janus monolayer transition-metal dichalcogenides," ACS Nano **11**(8), 8192–8198 (2017).
[40]A.-Y. Lu, H. Zhu, J. Xiao, C.-P. Chuu, Y. Han, M.-H. Chiu, C.-C. Cheng, C.-W. Yang, K.-H. Wei, and Y. Yang, "Janus monolayers of transition metal dichalcogenides," Nat. Nanotechnol. **12**(8), 744 (2017).

[41]J. O. Sofo, A. S. Chaudhari, and G. D. Barber, "Graphane: A two-dimensional hydrocarbon," Phys. Rev. B **75**(15), 153401 (2007).
[42]J. Zhou, Q. Wang, Q. Sun, X. Chen, Y. Kawazoe, and P. Jena, "Ferromagnetism in semihydrogenated graphene sheet," Nano Lett. **9**(11), 3867–3870 (2009).
[43]D. Haberer, C. E. Giusca, Y. Wang, H. Sachdev, A. V. Fedorov, M. Farjam, S. A. Jafari, D. V. Vyalikh, D. Usachov, and X. Liu, "Evidence for a new two-dimensional C_4H-type polymer based on hydrogenated graphene," Adv. Mater. **23**(39), 4497–4503 (2011).
[44]M. Yang, R. Zhao, J. Wang, L. Zhang, Q. Xie, Z. Liu, and Z. Liu, "Bandgap opening in Janus-type mosaic graphene," J. Appl. Phys. **113**(8), 084313 (2013).
[45]M. Yang, L. Zhou, J. Wang, Z. Liu, and Z. Liu, "Evolutionary chlorination of graphene: From charge-transfer complex to covalent bonding and non-bonding," J. Phys. Chem. C **116**(1), 844–850 (2012).
[46]J. T. Robinson, J. S. Burgess, C. E. Junkermeier, S. C. Badescu, T. L. Reinecke, F. K. Perkins, M. K. Zalalutdniov, J. W. Baldwin, J. C. Culbertson, and P. E. Sheehan, "Properties of fluorinated graphene films," Nano Lett. **10**(8), 3001–3005 (2010).
[47]R. Singh and G. Bester, "Hydrofluorinated graphene: Two-dimensional analog of polyvinylidene fluoride," Phys. Rev. B **84**(15), 155427 (2011).
[48]K. S. Novoselov, D. Jiang, F. Schedin, T. Booth, V. Khotkevich, S. Morozov, and A. K. Geim, "Two-dimensional atomic crystals," Proc. Natl. Acad. Sci. **102**(30), 10451–10453 (2005).
[49]Y. Cheng, Z. Zhu, M. Tahir, and U. Schwingenschlögl, "Spin-orbit–induced spin splittings in polar transition metal dichalcogenide monolayers," Europhys. Lett. **102**(5), 57001 (2013).
[50]B. Radisavljevic, A. Radenovic, J. Brivio, V. Giacometti, and A. Kis, "Single-layer MoS_2 transistors," Nat. Nanotechnol. **6**(3), 147 (2011).
[51]K. F. Mak, C. Lee, J. Hone, J. Shan, and T. F. Heinz, "Atomically thin MoS_2: A new direct-gap semiconductor," Phys. Rev. Lett. **105**(13), 136805 (2010).
[52]X. Xu, W. Yao, D. Xiao, and T. F. Heinz, "Spin and pseudospins in layered transition metal dichalcogenides," Nat. Phys. **10**(5), 343–350 (2014).
[53]K. F. Mak, K. He, J. Shan, and T. F. Heinz, "Control of valley polarization in monolayer MoS_2 by optical helicity," Nat. Nanotechnol. **7**(8), 494 (2012).
[54]F. Li, W. Wei, H. Wang, B. Huang, Y. Dai, and T. Jacob, "Intrinsic electric field-induced properties in Janus MoSSe van der Waals structures," J. Phys. Chem. Lett. **10**(3), 559–565 (2019).
[55]F. Li, W. Wei, P. Zhao, B. Huang, and Y. Dai, "Electronic and optical properties of pristine and vertical and lateral heterostructures of Janus MoSSe and WSSe," J. Phys. Chem. Lett. **8**(23), 5959–5965 (2017).
[56]A. Manchon, H. C. Koo, J. Nitta, S. Frolov, and R. Duine, "New perspectives for Rashba spin–orbit coupling," Nat. Mater. **14**(9), 871–882 (2015).
[57]K. Ishizaka, M. Bahramy, H. Murakawa, M. Sakano, T. Shimojima, T. Sonobe, K. Koizumi, S. Shin, H. Miyahara, and A. Kimura, "Giant Rashba-type spin splitting in bulk BiTeI," Nat. Mater. **10**(7), 521 (2011).
[58]Q.-F. Yao, J. Cai, W.-Y. Tong, S.-J. Gong, J.-Q. Wang, X. Wan, C.-G. Duan, and J. Chu, "Manipulation of the large Rashba spin splitting in polar two-dimensional transition-metal dichalcogenides," Phys. Rev. B **95**(16), 165401 (2017).
[59]M. A. U. Absor, H. Kotaka, F. Ishii, and M. Saito, "Tunable spin splitting and spin lifetime in polar WSTe monolayer," Jpn. J. Appl. Phys., Part 1 **57**(4S), 04FP01 (2018).
[60]B. Huang, G. Clark, E. Navarro-Moratalla, D. R. Klein, R. Cheng, K. L. Seyler, D. Zhong, E. Schmidgall, M. A. McGuire, and D. H. Cobden, "Layer-dependent ferromagnetism in a van der Waals crystal down to the monolayer limit," Nature **546**(7657), 270 (2017).
[61]C. Gong, L. Li, Z. Li, H. Ji, A. Stern, Y. Xia, T. Cao, W. Bao, C. Wang, and Y. Wang, "Discovery of intrinsic ferromagnetism in two-dimensional van der Waals crystals," Nature **546**(7657), 265 (2017).
[62]M. Bonilla, S. Kolekar, Y. Ma, H. C. Diaz, V. Kalappattil, R. Das, T. Eggers, H. R. Gutierrez, M.-H. Phan, and M. Batzill, "Strong room-temperature ferromagnetism in VSe_2 monolayers on van der Waals substrates," Nat. Nanotechnol. **13**(4), 289 (2018).
[63]D. J. O'Hara, T. Zhu, A. H. Trout, A. S. Ahmed, Y. K. Luo, C. H. Lee, M. R. Brenner, S. Rajan, J. A. Gupta, and D. W. McComb, "Room temperature intrinsic ferromagnetism in epitaxial manganese selenide films in the monolayer limit," Nano Lett. **18**(5), 3125–3131 (2018).
[64]Y. Deng, Y. Yu, Y. Song, J. Zhang, N. Z. Wang, Z. Sun, Y. Yi, Y. Z. Wu, S. Wu, and J. Zhu, "Gate-tunable room-temperature ferromagnetism in two-dimensional Fe_3GeTe_2," Nature **563**(7729), 94 (2018).
[65]Z. Fei, B. Huang, P. Malinowski, W. Wang, T. Song, J. Sanchez, W. Yao, D. Xiao, X. Zhu, and A. F. May, "Two-dimensional itinerant ferromagnetism in atomically thin Fe_3GeTe_2," Nat. Mater. **17**(9), 778 (2018).
[66]C. Zhang, Y. Nie, S. Sanvito, and A. Du, "First-principles prediction of a room-temperature ferromagnetic Janus VSSe monolayer with piezoelectricity, ferroelasticity, and large valley polarization," Nano Lett. **19**(2), 1366–1370 (2019).
[67]M. Moaied, J. Lee, and J. Hong, "A 2D ferromagnetic semiconductor in monolayer Cr-trihalide and its Janus structures," Phys. Chem. Chem. Phys. **20**(33), 21755–21763 (2018).
[68]J. Liang, M. Chshiev, A. Fert, and H. Yang, "Very large Dzyaloshinskii-Moriya interaction in two-dimensional Janus manganese dichalcogenides and its application to realize field-free skyrmions," preprint arXiv:1906.00648 (2019).
[69]J. Yuan, Y. Yang, Y. Wu, Y. P. Feng, Y. Chen, X. Yan, and L. Shen, "Zero-field sub-50-nm skyrmions in monolayer Janus Van der Waals magnets," preprint arXiv:1906.10836 (2019).
[70]J. R. Schaibley, H. Yu, G. Clark, P. Rivera, J. S. Ross, K. L. Seyler, W. Yao, and X. Xu, "Valleytronics in 2D materials," Nat. Rev. Mater. **1**(11), 16055 (2016).
[71]C. Xia, W. Xiong, J. Du, T. Wang, Y. Peng, and J. Li, "Universality of electronic characteristics and photocatalyst applications in the two-dimensional Janus transition metal dichalcogenides," Phys. Rev. B **98**(16), 165424 (2018).
[72]A. C. Riis-Jensen, M. Pandey, and K. S. Thygesen, "Efficient charge separation in 2D Janus van der Waals structures with built-in electric fields and intrinsic p–n doping," J. Phys. Chem. C **122**(43), 24520–24526 (2018).
[73]L. Dong, J. Lou, and V. B. Shenoy, "Large in-plane and vertical piezoelectricity in Janus transition metal dichalchogenides," ACS Nano **11**(8), 8242–8248 (2017).
[74]W. Shi and Z. Wang, "Mechanical and electronic properties of Janus monolayer transition metal dichalcogenides," J. Phys.: Condens. Matter **30**(21), 215301 (2018).
[75]C. H. Naylor, W. M. Parkin, J. Ping, Z. Gao, Y. R. Zhou, Y. Kim, F. Streller, R. W. Carpick, A. M. Rappe, and M. Drndic, "Monolayer single-crystal 1T′-$MoTe_2$ grown by chemical vapor deposition exhibits weak antilocalization effect," Nano Lett. **16**(7), 4297–4304 (2016).
[76]Z. Fei, T. Palomaki, S. Wu, W. Zhao, X. Cai, B. Sun, P. Nguyen, J. Finney, X. Xu, and D. H. Cobden, "Edge conduction in monolayer WTe_2," Nat. Phys. **13**(7), 677 (2017).
[77]Y. Wang, J. Xiao, H. Zhu, Y. Li, Y. Alsaid, K. Y. Fong, Y. Zhou, S. Wang, W. Shi, and Y. Wang, "Structural phase transition in monolayer $MoTe_2$ driven by electrostatic doping," Nature **550**(7677), 487 (2017).
[78]Z. Wang, "2H → 1T′ phase transformation in Janus monolayer MoSSe and MoSTe: An efficient hole injection contact for 2H-MoS_2," J. Mater. Chem. C **6**(47), 13000–13005 (2018).
[79]X. Tang, S. Li, Y. Ma, A. Du, T. Liao, Y. Gu, and L. Kou, "Distorted Janus transition metal dichalcogenides: Stable two-dimensional materials with sizable band gap and ultrahigh carrier mobility," J. Phys. Chem. C **122**(33), 19153–19160 (2018).
[80]M. Yagmurcukardes, C. Sevik, and F. Peeters, "Electronic, vibrational, elastic, and piezoelectric properties of monolayer Janus MoSTe phases: A first-principles study," Phys. Rev. B **100**(4), 045415 (2019).
[81]A. Pant, Z. Mutlu, D. Wickramaratne, H. Cai, R. K. Lake, C. Ozkan, and S. Tongay, "Fundamentals of lateral and vertical heterojunctions of atomically thin materials," Nanoscale **8**(7), 3870–3887 (2016).
[82]S. Tongay, H. Sahin, C. Ko, A. Luce, W. Fan, K. Liu, J. Zhou, Y.-S. Huang, C.-H. Ho, and J. Yan, "Monolayer behaviour in bulk ReS_2 due to electronic and vibrational decoupling," Nat. Commun. **5**, 3252 (2014).
[83]C. Yu, X. Cheng, C. Wang, and Z. Wang, "Tuning the n-type contact of graphene on Janus MoSSe monolayer by strain and electric field," Physica E **110**, 148–152 (2019).
[84]T. Jing, D. Liang, J. Hao, M. Deng, and S. Cai, "Interface Schottky barrier in Hf_2NT_2/MSSe (T = F, O, OH; M = Mo, W) heterostructures," Phys. Chem. Chem. Phys. **21**(10), 5394–5401 (2019).
[85]Z. Kahraman, A. Kandemir, M. Yagmurcukardes, and H. Sahin, "Single-layer Janus-type platinum dichalcogenides and their heterostructures," J. Phys. Chem. C **123**(7), 4549–4557 (2019).

[86]H. Liu, Z. Huang, C. He, Y. Wu, L. Xue, C. Tang, X. Qi, and J. Zhong, "Strain engineering the structures and electronic properties of Janus monolayer transition-metal dichalcogenides," J. Appl. Phys. **125**(8), 082516 (2019).
[87]Y. Zhang, H. Ye, Z. Yu, Y. Liu, and Y. Li, "First-principles study of square phase MX_2 and Janus MXY (M = Mo, W; X, Y = S, Se, Te) transition metal dichalcogenide monolayers under biaxial strain," Physica E **110**, 134–139 (2019).
[88]W. Zhou, J. Chen, Z. Yang, J. Liu, and F. Ouyang, "Geometry and electronic structure of monolayer, bilayer, and multilayer Janus WSSe," Phys. Rev. B **99**(7), 075160 (2019).
[89]A. Kandemir and H. Sahin, "Bilayers of Janus WSSe: Monitoring the stacking type via the vibrational spectrum," Phys. Chem. Chem. Phys. **20**(25), 17380–17386 (2018).
[90]X. Liu, H. Zhou, B. Yang, Y. Qu, and M. Zhao, "Strain-modulated electronic structure and infrared light adsorption in palladium diselenide monolayer," Sci. Rep. **7**, 39995 (2017).
[91]S. Tao, B. Xu, J. Shi, S. Zhong, X. Lei, G. Liu, and M. Wu, "Tunable dipole moment in Janus single-layer MoSSe via transition-metal atom adsorption," J. Phys. Chem. C **123**(14), 9059–9065 (2019).
[92]R. Peng, Y. Ma, S. Zhang, B. Huang, and Y. Dai, "Valley polarization in Janus single-layer MoSSe via magnetic doping," J. Phys. Chem. Lett. **9**(13), 3612–3617 (2018).
[93]H. Cai, J. Kang, H. Sahin, B. Chen, A. Suslu, K. Wu, F. Peeters, X. Meng, and S. Tongay, "Exciton pumping across type-I gallium chalcogenide heterojunctions," Nanotechnology **27**(6), 065203 (2016).
[94]P. Hu, J. Zhang, M. Yoon, X.-F. Qiao, X. Zhang, W. Feng, P. Tan, W. Zheng, J. Liu, and X. Wang, "Highly sensitive phototransistors based on two-dimensional GaTe nanosheets with direct bandgap," Nano Res. **7**(5), 694–703 (2014).
[95]M. Yagmurcukardes, R. Senger, F. Peeters, and H. Sahin, "Mechanical properties of monolayer GaS and GaSe crystals," Phys. Rev. B **94**(24), 245407 (2016).
[96]D. A. Bandurin, A. V. Tyurnina, L. Y. Geliang, A. Mishchenko, V. Zólyomi, S. V. Morozov, R. K. Kumar, R. V. Gorbachev, Z. R. Kudrynskyi, and S. Pezzini, "High electron mobility, quantum Hall effect and anomalous optical response in atomically thin InSe," Nat. Nanotechnol. **12**(3), 223 (2017).
[97]Y. Guo, S. Zhou, Y. Bai, and J. Zhao, "Enhanced piezoelectric effect in Janus group-III chalcogenide monolayers," Appl. Phys. Lett. **110**(16), 163102 (2017).
[98]A. Kandemir and H. Sahin, "Janus single layers of In_2SSe: A first-principles study," Phys. Rev. B **97**(15), 155410 (2018).
[99]Y. Bai, Q. Zhang, N. Xu, K. Deng, and E. Kan, "The Janus structures of group-III chalcogenide monolayers as promising photocatalysts for water splitting," Appl. Surf. Sci. **478**, 522–531 (2019).